THE ROLE OF PKC-γ IN REGULATING LENS GAP JUNCTION COUPLING

Satyabrata Das[1], Francisco J. Martinez-Wittinghan[2], Huan Wang[2], Dolores J. Takemoto[1], Guido Zampighi[3], Richard Mathias[2]
[1]Department of Biochemistry, Kansas State University, Kansas; [2]Department of Physiology and Biophysics, State University of NY, Stony Brook, NY;
[3]Department of Neurobiology, Jules Stein Eye Research Institute University of California, Los Angeles School of Medicine, Los Angeles, CA

The American Society for Cell Biology 48th Annual Meeting December 13-17, 2008 • San Francisco

Abstract

Objectives. In the lens, activation of PKCγ with phorbol esters has been reported to phosphorylate connexins and down regulate gap junction coupling. To determine whether PKCγ has a role in regulation of gap junction coupling in the normal lens, we have compared the properties of coupling in lenses from wild type (WT) and PKCγ knockout (KO) mice.

Methods. Gap junction protein expression was studied using western blotting; gap junction structure was observed using thin section electron microscopy; gap junction coupling conductance was measured in intact lenses using impedance studies.

Results. There were no gross differences in size or clarity or expression of Cx46 or Cx50 in lenses from WT and PKCγ KO mice. However, in WT lenses, Cx43 is found only in epithelial cells whereas in PKCγ KO lenses, expression continues into the fiber cells, with the highest levels in the outer differentiating fibers (DF) but some detectable protein in the inner mature fibers (MF). DF and to some extent MF of PKCγ KO lenses contained vesicular like structures that were formed from two membranes connected by a gap junction. These structures could be invaginations of cell to cell junctions that were sectioned and thus appeared vesicular, or internalized junctions on their way to degradation. In either case they represent a large increase in the area of gap junctions over that seen in WT lenses. These structures were never seen in WT lenses. Gap junction coupling conductance in the DF of PKCγ KO lenses was 19% larger than that of WT. In the MF, the effect was much larger with the KO lenses having a 253% increase in coupling over WT.

Conclusions. PKCγ has a major role in the regulation of gap junction expression and coupling in the normal lens. The most dramatic effects of PKC-γ KO on Cx43 expression and cellular structure occurred in the DF whereas the most dramatic increase in coupling conductance occurred in the MF, where Cx46 is thought to solely mediate coupling. Perhaps Cx46 is normally phosphorylated by PKCγ, which inhibits the number of open channels.

Methods

Animals: All animal procedures were approved by Kansas State University Institutional Animal Care and Use Committee. Wild type (WT) and PKCγ knock-out mice (KO) were obtained from Jackson Laboratories (Bar Harbor, MA, USA) . All mice were genotyped by PCR of tail snips prior to all experiments. Only homozygous KO mice were used for experiments. Mice were sacrificed by CO_2 followed by cervical dislocation.

Lens: Mouse lenses were surgically removed from WT and KO eyeballs. Lenses were then homogenized or dissected into outer, cortical and nuclear regions followed by western blotting.

Tissue Culture : N/N 1003A rabbit lens epithelial cells were grown in DMEM with 10% fetal bovine serum until 90% confluent followed by treatment with 400nm TPA for up to 24 hours. After that lens cells were collected and homogenized by sonication and the whole cell homogenate was used for Western blotting (WB) to analyze protein composition.

Western Blot (WB): Proteins were electrophoretically transferred from gels to nitrocellulose membranes. The membranes were blocked in 5% nonfat milk in phosphate-buffered saline with 0.1% Tween-20 and probed with antibodies at 2 μg/mL overnight. Species specific secondary antibodies, conjugated with horse radish peroxidase followed by x-ray to detect chemoluminescence were used to visualize specific bands. UN-SCAN-IT gel and graph digitizing software (Silc Scientific, Orem, Utah, USA) was used to digitize bands.

Conical Tomography: Tomographic series in conical geometry were collected with the specimens tilted at 55° and rotated by 5° until completing a 360° turn. They were aligned using fiduciary points, reconstructed with the weighted back projection algorithm, and analyzed by density segmentation using the watershed algorithm (Salvi et al., 2008).

Freeze-Fracture: Bundles of fibers (5-7 fibers) were rapidly frozen (avoiding any cross-linking with chemical fixatives) and fractured in a JOEL freeze-fracture apparatus. The cleaved surfaces were shadowed with platinum-carbon at 70° and carbon at 90° (Zampighi et al., 2005).

Impedance Studies: Mice were sacrificed by injection with sodium pentobarbitone solution (100 mg/kg of weight). The dissected lenses were placed in Tyrode solution (137.7 mM NaCl; 5.4 mM KCl; 2.3 mM NaOH; 1 mM $MgCl_2$; 10 mM glucose; 5 mM Hepes; pH 7.4). To perform impedance studies, microelectrodes were shielded with the silver paint to near the tip and also coated with silicone (silicone elastomer base: silicone elastomer curing agent: 10:1). The function of the silicone was to avoid the grounded silver paint contacting the bath. One microelectrode (current electrode, I in Fig 5) was used to inject a current into a lens central fiber cell. The second microelectrode (voltage electrode, V in Fig 5) was used to record the induced voltage. The voltage electrode was placed into the lens at different depths. Impedance was calculated by a fast Fourier analyzer. R_s (series resistance see Fig 6) was used to evaluate gap junction coupling.

Methods

Model of Gap Junctional Coupling: At sinusoidal frequencies approaching 1 kHz, the induced intracellular and extracellular voltages become nearly identical and are given by V = IRs, where I is the injected current and R_s (Ω) (shown in Fig 6) is the cumulative series resistance between the point of voltage recording (*r* cm from the center), and the lens surface (*a* cm from the center). R_s is directly proportional to the parallel resistivity of the intracellular and extracellular compartments (R_p, Ωcm).

$$R_s = \frac{1}{4\pi}\int_r^a \frac{R_p}{\rho^2}\,d\rho, \qquad (1)$$

$$R_p = \frac{R_i R_e}{R_i + R_e}$$

The effective intracellular resistivity, R_i is due mainly to the gap junctional coupling resistance whereas the effective extracellular resistivity, R_e, depends on the tortuosity and volume fraction of small extracellular clefts. In normal physiological conditions, R_e is much higher than R_i, therefore $R_p \approx R_i$. Our data suggest R_e is uniform, whereas we have measured that R_i changes at the DF to MF transition (defined as *r = b*). Integrating Eq. 1 gives:

$$R_s = \frac{R_{DF}}{4\pi}\left(\frac{1}{r}-\frac{1}{a}\right) \qquad b \le r \le a \qquad (2)$$

$$R_s = \frac{R_{DF}}{4\pi}\left(\frac{1}{b}-\frac{1}{a}\right)+\frac{R_{MF}}{4\pi}\left(\frac{1}{r}-\frac{1}{b}\right) \qquad r \le b \qquad (3)$$

where RDF is Ri in DF and RMF is Ri in MF. Eq 2 or 3 was curve fit to the RS data to obtain values of RDF and RMF. Fiber cells are approximately 3 μm wide, so the coupling conductance per area of cell to cell contact was calculated as 1/(3x10-4Ri).

References

1. Salvi et al. (2008) J Struct Biol 161:287–297
2. Zampighi et al. (2005) J Struct Biol. 151(3):263-74.

Degradation of Cx43 and not Cx50 by PKCγ activation in N/N Cells

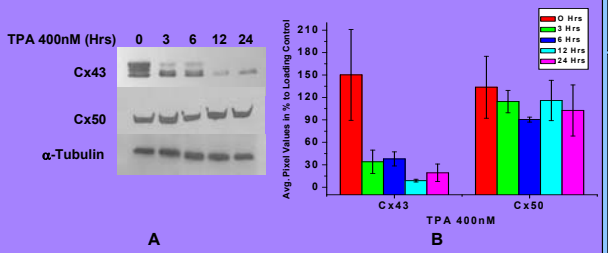

Figure 1. (A) – Western blot analyses of Cx43 and Cx50 in N/N cell homogenate after treatment with 400 nM TPA for different time periods (0-24 Hrs). Long term exposure of the lens epithelial cells to TPA resulted in the degradation of Cx43, where as it had no effect on Cx50. α-Tubulin was used as a loading control. (**B**) – The average pixel values for every Cx43 and Cx50 band was calculated, then normalized and plotted in % of loading control (α-Tubulin). UN-SCAN-IT gel and graph digitizing software (Silc Scientific, Orem, Utah) was used to digitize bands.

Distribution of PKCγ in the Control Lenses

Figure 2. Lenses were collected from wild type mice and dissected into outer, cortical, and nuclear regions, then homogenized in cell lysis buffer, sonicated, and sample loading buffer was added. Then the different samples were immunoblotted with anti-PKCγ antibody. PKCγ was found to be present in all three regions of the lens, whereas PKCγ was absent from the PKCγ knock-out mouse lens (Figure not shown).

Distribution of Cx43 in Control and PKCγ KO lenses

Figure 3. Western blot analyses of Cx43 in homogenates of freshly isolated wild type and PKCγ knock out lenses; dissected into outer, cortical, and nuclear regions. In the wild type mouse lenses, Cx43 was present only in the outer region in the epithelial cells, whereas in the PKCγ knock out mouse lenses Cx43 persisted into the cortical region. The distribution of Cx46 and Cx50 were identical both in the wild type and PKCγ knock out mouse lens (not shown).

Total Cx43 & Cx50 Protein Levels

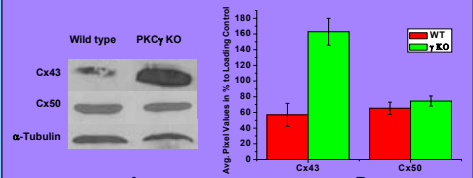

Figure 4. (A) – Western blot analyses of Cx43 and Cx50 in total lens homogenates of freshly isolated wild type and PKCγ knock out lenses. α-Tubulin was used as a loading control. **(B)** – The average pixel values for every Cx43 and Cx50 band was calculated, then normalized and plotted in % of loading control (a-Tubulin). UN-SCAN-IT gel and graph digitizing software (Silc Scientific, Orem, Utah) was used to digitize bands. The PKCγ knock out mouse lens has ~100% more total Cx43 than the control lens.

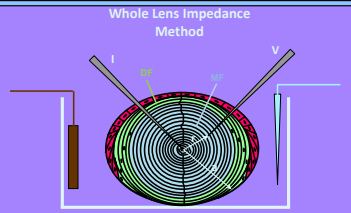

Figure 5

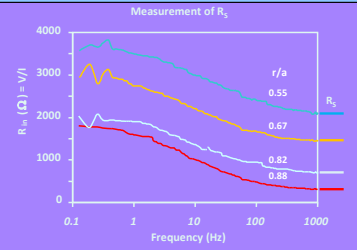

Figure 6

R_S Data and Curve Fits From PKCγ KO and WT Lenses

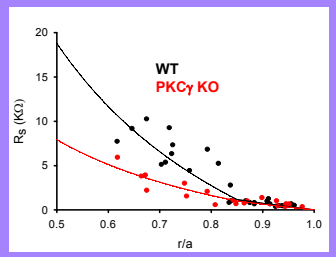

Figure 7. The WT data were from 11 lenses taken from 7 mice. The KO data were from 9 lenses taken from 5 mice. The mice were approximately 9 months old. In each lens, one measurement of R_S in the DF was made, then the voltage microelectrode was advanced into the MF where R_S was determined at one or more locations. The values of R_S in the WT lenses are clearly higher than those in PKCγ KO lenses, suggesting PKCγ down regulated gap junction coupling.

Comparison of Transport Properties

		WT	PKCγ KO
Radius	cm	0.13±0.003	0.13±0.002
Input Resistance	KΩ	2.9±1.7	3.4±1.5
Resting Voltage	mV	-54±6	-53±5
Coupling Conductance	S/cm^2	0.31	0.37
	S/cm^2	0.10	0.25
Normalized Coupling Conductance	-	1	1.19*
	-	1	2.50*

Table 1. A comparison of transport properties of lenses from PKCγ KO and WT mice. There were no significant differences in radii, resting voltages and input resistances (the impedance at 0 Hz). All lenses were transparent. In PKCγ KO lenses, however, the average coupling conductance was significantly higher than in WT lenses (*P < 0.05). This was particularly evident in the inner core of MF where the coupling conductance of PKCγ KO lenses was elevated by 250% over that of WT lenses.

Gap Junctions in the PKC-γ KO lens (2-weeks-old mice)

Figure 8. Panel A shows a low magnification view of cortical fiber cells in the mouse lens. The areas inside the rectangle and indicated by the arrow represent extensive gap junctions connecting adjacent fiber cells. Panel B shows a view of the P (protoplasmic) face of the fiber plasma membrane. The regions colored pink indicate gap junction plaques. Bar: 0.6 μm.

Ablation of PKC-γ induces "reflective" gap junctions in lens fiber cells.

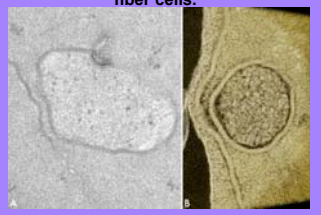

Figure 9. Panel A shows a higher magnification view of the two types of gap junctions in cortical fiber cells. One type connects the plasma membranes of adjacent fibers (arrow). The other type is the "reflective" gap junction that appears as a large diameter vacuole in the fiber's cytoplasm. Occasionally, these gap junction vacuoles are continuous with the plasma membrane and might participate in cell-to-cell communication. "Reflective" gap junctions do not exist in fibers of wild type animals. Panel B is a 3D-reconstruction of a region exhibiting both types of gap junctions. Bar: 0.2 μm.

Conclusions

- **PKCγ has a major role in the regulation of gap junction protein, Cx43, location and degradation.**
- **The PKCγ KO mice lens has ~100% more total Cx43 on average than the control mice lens and Cx43 persists into the cortical region of the lens in PKCγ KO mice, whereas it is found only in the outer epithelial region in WT mice. Loss of PKCγ does not alter CX50 and Cx46 distribution or protein levels.**
- **The most dramatic effects of PKCγ KO on Cx43 expression and cellular structure occurred in the cortical region whereas the most dramatic increase in coupling conductance occurred in the MF, where Cx46 is thought to solely mediate coupling. Perhaps Cx46 is normally phosphorylated by PKCγ, which inhibits the number of open channels.**